HISTORIA NATURAL

Tercera Serie | Volumen 11 (2) | 2020/17-37

GEOPHYSICAL CONSTRAINTS OF THE RIO DE LA PLATA'S *ARCHON* CRATON

Contrastes geofísicos del Cratón Archon Rio de la Plata

Jaime L.B. Presser[1] and Pedro Benítez[2]

[1]JP-Exploraciones. Mbocaya y Concepción, Asunción, Paraguay. jaimeleonardobp@yahoo.es
[2]Paraguari, Paraguay. pbenittez@hotmail.com

AZARA
FUNDACIÓN DE HISTORIA NATURAL

umai Universidad Maimónides

Abstract. We are delineating with geophysics, between Paraguay, Argentina, Uruguay and Brazil, the edges of the Rio de la Plata SCLM *Archon* Craton. For the geophysics constraint we focused on the published data of S-wave (% dVs TX2011 3-D a global mantle shear-wave tomography model) that is complemented with the published P-wave (% dVp continental, SAM5_P_2019 3-D Tomographic Earth Model). Edges that are reinforced by the gravimetry (WGM2012 GLOBAL MODEL); crustal thickness (mostly 41 km thick; that is thinning to the SSE); magnetometry (combination of EMAG, WDMAM 2, and Compilation Getech); and peridotitic mantle geotherm information (characterized by cratonic values 38.5/39-40 mW/m^2 bordered east by, irregularly, by a strip of 41 mW/m^2 and it is weathered by 42-44.5 mW/m^2; while the to west side denote typically non-cratonic values as ≥45 mW/m^2). The tomographic S-wave and so as the P-wave define a seismically craton-keel that extends to depths of ~280-300 km.¸ that are in general agreement with regional studies of several other *Archon* cratonic regions. The inferred geotherm data for the Rio de la Plata SCLM *Archon* Craton project keel thicknesses as great as 213 to 243 km depth. The Rio de la Plata SCLM *Archon* Craton hosts abundant diamond-bearing lamproitic pipes, diamond-bearing picritic calc-alkaline lamprophyres pipes (Paraguay), and diamond-bearing ultramafic lamprophyres (Uruguay).

Key word. Rio de la Plata SCLM *Archon* Craton, S-wave, P-wave, peridotitic mantle geotherm, diamond-bearing lamproitic pipes, diamond-bearing lamprophyres.

Resumen. Se ha delineando con geofísica, entre Paraguay, Argentina, Uruguay y Brasil, los bordes del SCLM Cratón *Archon* Río de la Plata. La definición geofísica, se centró en los datos publicados de la onda S (% dVs TX2011 3-D, un modelo de tomografía de ondas-S del manto global) la que se complementa con los datos publicados de ondas-P (% dVp continental, SAM5_P_2019 3-D Modelo Tomográfico Terrestre). Los bordes han sido reforzados con la gravimetría (MODELO GLOBAL WGM2012); espesor de la corteza (mayormente de 41 km de espesor; que se adelgaza al SSE); magnetometría (combinación de EMAG, WDMAM 2 y Compilación Getech); e información geotérmica del manto peridotítico (este se caracteriza por valores cratónicos 38.5/39-40 mW/m^2 bordeado al este, irregularmente, por una franja de 41 mW/m^2 y esta a su ver por 42-44.5 mW/m^2; mientras que el lado oeste denota típicamente valores no cratónicos ≥45 mW/m^2). Las ondas tomográficas S y P definen raíz sísmica cratónica que se extiende a profundidades de ~280-300 km. Datos que están en general de acuerdo con estudios regionales de varias otras regiones cratónicas *Archon*. Los datos de geotermia inferidos para el proyectado del SCLM Cratónico *Archon* Río de la Plata infieren espesores de raíz-cratónica de hasta 213 a 243 km de profundidad. El SCLM Cratónico *Archon* Río de la Plata alberga abundantes *pipes* lamproíticos con diamantes, *pipes* de lamprófidos calco-alcalinos picríticos con diamantes (Paraguay) y lamprófidos ultramáficos con diamantes (Uruguay).

Palabras clave. Rio de la Plata SCLM *Archon* Craton, S-Wave, P-Wave, geotermia peridotitica del manto; *pipes* lamproíticos con diamantes, *pipes* de lamprófidos con diamantes.

INTRODUCTION

Janse (1994) proposed a simple classification of cratons into three major divisions, i.e. *Archons*, *Protons*, and *Tectons*. Cratons were interpreted in the broadest sense in that they include Archaean cores or nuclei as well as Paleoproterozoic, Mesoproterozoic, and Neoproterozoic mobile belts. This whole assemblage often carries a bewildering array of local stratigraphic and tectonic names so that it is confusing for a geologist, not familiar with the area, to understand the tectonic pattern. This is important for diamond exploration as economic kimberlites occur only in areas underlain by Archaean basement, termed Archons, which in most cases infers a thick lithosphere (Janse, 1994 and 1998).

Begg *et al.* (2009) modify the Janse (1998) cratons terminology, in which the last major crustal tectonthermal event in *Archons* occurred at ≥2.5 Ga (Archaeozoic), in *Protons* between 2.5 and 1 Ga (Lower to Middle Proterozoic), and in *Tectons* at <1 Ga (Upper Proterozoic).

Regarding the craton deep view, the specifics of the study of the Earth's deep interior, including the lithosphere, is that all of the parameters measured in direct and indirect geophysical and geochemical surveys are interrelated, being strongly dependent (among other factors) on pressure, temperature, composition, and the physical state of matter. This necessitates joint interpretation of the entire set of data provided using different techniques in the Earth sciences (such as seismic, gravity, thermal, electromagnetic, and petrological) (Artemieva, 2011).

The lithosphere is the outermost, relatively rigid shell of the Earth, made up of the crust and the underlying lithospheric mantle. Beneath the continents, the subcontinental lithospheric mantle (SCLM) varies widely in thickness, from a few tens of kilometers beneath active rift zones to >250 km beneath some ancient (*Archon*) cratonic blocks (Begg *et al.,* 2009). Presser (2011), states that the LAB (Lithosphere asthenosphere boundary) depth greater than 193.5 at 195 km would denote ages> 2500 Ma., this estimated from the formula $z = 0.04 * t + 93.6$ (Artemieva, 2006, see also Artemieva, 2011); where t is the age in millions of years. Understanding the formation and evolution of *Archon* cratons remains one of the holy grails of earth science (Fouch *et al.,* 2004 and references).

The SCLM, as sampled by xenoliths in volcanic rocks and some exposed massifs, consists almost entirely of peridotitic rocks (olivine + orthopyroxene ± garnet ± clinopyroxene ± spinel). Re-Os isotopic studies show that beneath some *Archons* cratons, the SCLM is at least as old as the oldest known crustal rocks (Begg *et al.,* 2009 and references). *Archon* SCLM is strongly depleted in basaltic components, with highly Magnesian olivine and pyroxenes, whereas *Tecton* SCLM is only mildly depleted relative to estimates of primitive mantle compositions; *Proton* SCLM tends to be intermediate between these two extremes (Begg *et al.,* 2009).

As can be appreciated in the works of Rocha (2003), Rocha *et al.* (2011, 2016, and 2019), Chaves *et al.* (2016) and so as, Azevedo (2017); seismic (S and P-wave), constraints higher, craton-like, velocities beneath of Central South America indicating that the probable *Archon* Craton lies along the northern boundary of these terranes. So, in this work we integrating geophysical data (Seismic, geotherm, gravity, and magnetic) to constraints this probable Cratonic SCLM from Central- South America; on this occasion a refined limit that will be presented and discussed in this paper, this as an update to the previous suggestions that are shown in Presser (2016c, 2019 and 2020) as well as by Presser *et al.* (2017) Presser and Benitez (2021).

METHODOLOGY

For S-wave data we employed the (Body waves) TX2011 3-D Tomographic Earth Model, A global mantle shear-wave tomography model from Grand, (2002) available in: http://ds.iris.edu/ds/products/emc-tx2011/ (consulted in 2015-2021). Available also in: https://www.earth.ox.ac.uk/~smachine/cgi/index.php?page=cross_section.

For P-wave data we used the (Body waves) SAM5_P_2019 3-D Tomographic Earth Model, Relative P-wave velocity (%dVp) from Portner *et al.* (2019) available in: http://ds.iris.edu/ds/products/emc-sam5_p_2019/ (consulted in April, 2021). Available also in: https://www.earth.ox.ac.uk/~smachine/cgi/index.php?page=cross_section.

We were estimated the geotherms at 150 km depth used the Moulik and Ekstrom (2014) model, which shows 3-degree spacing, the software used in Iris (http://ds.iris.edu/dms/products/emc/depth_profile.html) would achieve a very acceptable extrapolation of the data (*cf.* comments in Presser, 2020 and Presser and Benitez, 2021).

For configuration the Crustal Thickness we used LITHO1.0; Lithospheric Model of the Earth extracted from: https://igppweb.ucsd.edu/~gabi/litho1.0.html (consulted in March 2021).

In the Gravimetric Constraints we used data of WGM2012 GLOBAL MODEL(Bonvalot *et al.*, 2012)available in: https://bgi.obs-mip.fr/data-products/grids-and-models/wgm2012-global-model/ (consulted in February 2021).

For Magnetometric constraints we used the global data EMAG or Earth Magnetic Anomaly Grid (https://www.ngdc.noaa.gov/geomag/emag2.html); WDMAM (http://wdmam.org/download.php#downloadmodel./WDMAM 2 (Lesur *et al.*, 2016) and Compilation Getech (https://getech.com/getech-products/content/magnetic-data/).

RESULTS

Seismic Constraints

Teleseismic travel time tomography is one of the most widely used techniques to image the 3D velocity structure of the lithosphere and uppermost upper mantle. Its popularity resides in the relatively low cost of passive seismic deployments, the high horizontal resolution (on the scale of tens of kilometers) that can be achieved, its applicability to regions with no local seismicity, and the high-quality data that can be extracted from the array using cross-correlation techniques (Afonso *et al.*, 2016 and references).

In diamond geology, the greatest exact approximation of the limits or the domain of an *Archon* Cratonic SCLM is achieved with geophysical tools; especially with the use of S-wave that is complemented with P-wave (*cf.* James *et al.*, 2001, 2004; Fouch *et al.*, 2004; Begg *et al.*, 2009; Artemieva, 2011; Faure *et al.*, 2011**;** Presser, 2011, 2016c, 2019 and 2020; Presser *et al.*, 2017; Celli *et al.*, 2020; Chaves *et al.*, 2016; Assumpção *et al.*, 2017).

S-wave and P-wave.

The information on both Vs and Vp waves is particularly useful when making inferences about the thermochemical structure of the Earth (*cf.* Afonso *et al.*, 2016 and references). While surface wave data provide essential constraints on the absolute 3D velocity structure, (Afonso *et al.*, 2016). In this regard, beneath Cratonic SCLM from South America, we stand out works of Schimmel *et al.* (2003), Assumpção *et al.* (2004), Roccha (2003) Rocha *et al.* (2011, 2016 and 2019), Azevedo *et al.* (2015), Rosa *et al.* (2016), Affonso *et al.* (2019) and others.

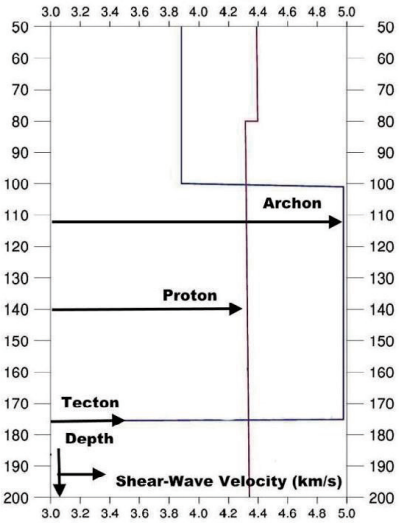

Figure 1 - 1D of the S-waves (expressed as dVs% of the model TX2011 *vs* PREM) on the different tectonic environments of cratonic lithospheric mantles: archon, proton and tecton. *Archon* lithospheric mantles: can be identified by very high velocity =dVs% greater than 4.3-4.4 in relation to the PREM (between 100-175km depth); from Presser (2020); Presser and Kumar (2020). Seismic information source from: http://ds.iris.edu/dms/products/emc/horizontalSlice.html, the Iris page.

Presser (2020; see also, Presser and Kumar, 2020) based on the behavior 1D of the S-waves expressed as dVs% of the TX2011 3-D Tomographic Earth Model vs PREM (cf. http://ds.iris.edu/dms/products/emc/horizontalSlice.html), on the different kimberlites and lamproites in the *Archon*, *Proton*, and *Tecton* lithospheric mantles (Figure 1), affirmed that all diamond mines with a high degree of diamonds (greater than 100 pht) occurred only in *Archon* lithospheric mantles: i.e. lithospheric mantle with very high velocity (dVs% greater than 4.3-4.4 about the PREM in 1D profiles, between 100-175 km depth) (Figure 1). When this is taken as a global model at 150 km depth of 2D seismic tomographic of the dVs% model TX2011 and in the delimited domains superior/equal to 4.3 dVs% and the area covered by all the (rich and world-class) diamond mines (of kimberlites and lamproites) the criterion shows good agreement (Figure 2), Presser (2020). So, this information we used to delimit/configure the probable SCLM *Archon* Craton Mantle.

Figure 3 Illustrates the delimitation of

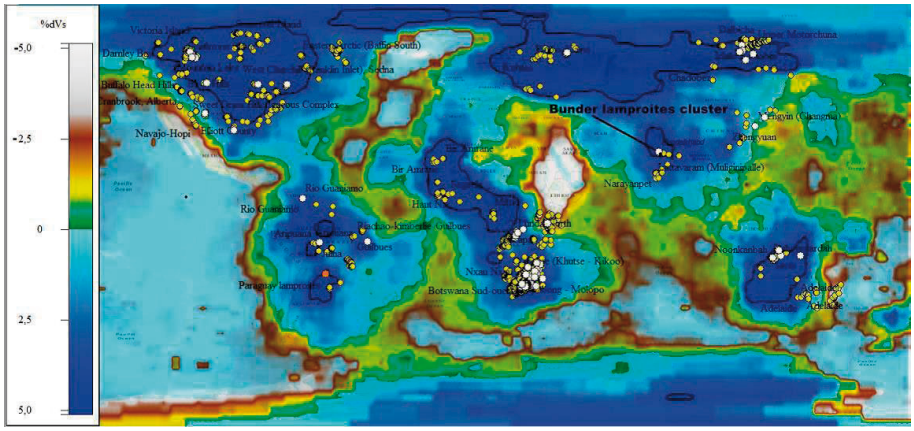

Figure 2 - Global (seismic configuration) *Archon* lithospheric mantles here delimited by iso-lines on a global map of % dVs at 150 km depth of the model TX2011. All the diamond mines (white balls), more especially those with greater than 100 cpht, are located within the delimited Archon lithospheric mantles. Area that is understood to be undisturbed over time and that could represent the core of the craton; this is archon-core. This refers to a lithospheric mantle that may or may not coincide with that found by surface geology in shield areas (Presser, 2020; Presser and Kumar, 2020). Seismic information source from the Iris page.

the inferred Cratonic SCLM beneath Central South America; this from dVs% of the Tomography TX2011 model. The 3 upper sheets of Figure 3 represent, from left to right: dVs% isolines at 150 km depth. In the middle, for the greater blue zone or high-speed dVs zone, is highlighting, in dashed, the isoline 4.3%; area as indicated by Presser (2020) they delimited domains of typically *Archon* of SCLM; i.e. Cratonic SCLM. The following figure highlights the edges of this Cratonic SCLM that has been carefully adjusted with 2D profiles and horizontal plate of the same dVs% information at 150 km depth. This Cratonic SCLM delimited area is sensed as being the Cratonic SCLM heart of the Rio de la Plata Craton; which from now on will be referred to simply as the Rio de la Plata SCLM Craton environment. It is followed by two other speed plates dVs% at 200 and 300 km depth in the same Figure 3. In both plates, a decrease dVs% velocity is noted for the Rio de la Plata SCLM Craton environment. A near slower speed is especially noticeable in the northern part of the Rio de la Plata SCLM Craton environment. In this area of the Rio de la Plata SCLM Craton environment, the works of Rocha (2003) and Rocha *et al.*, (2011) show that high % S-wave, speeds extend to a depth of around 1,100 km.

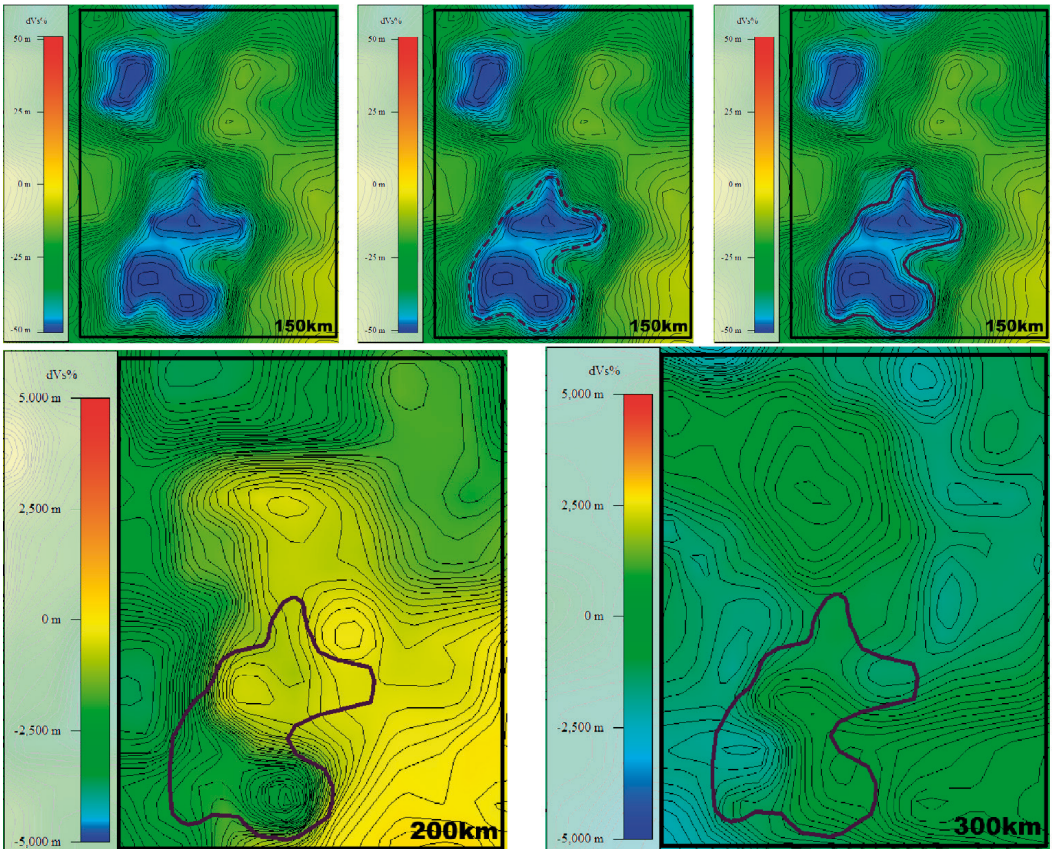

Figure 3 - The panel is a map of Vs velocity perturbations (TX2011 Tomography model) at 150 km depth (blue-zone) –superior; to 200 and 300 Km depth, below. The 3 upper figures at 150 km depth represent, from left to right: dVs% isolines at 150 km depth; the dashed line represents the 4.3 dVs%, and the thick line represents the delimitation (slightly adjusted the above) of the inferred Cratonic SCLM beneath Central South America.

P-wave, many authors have successfully used this approach to study crustal and shallow mantle structures (Afonso *et al.*, 2016). P-wave also would allow the inferences of an *Archon* Cratonic SCLM of being depleted or enriched, for example, Shirey *et al.* (2002), James and Fouch (2002), James *et al.* (2004), and also Begg *et al.* (2009).

Figure 4 illustrates the P-wave velocity perturbations at 130 km, 200 km, and 300 Km depth (% dVp Tomography model SAM5_P_2019 of Portner *et al.*, 2020), area as in Figure 3, in relation to the Rio de la Plata SCLM Craton environment. At 130 km and 200 km there are some high-speed islands and at 300 km standing out at the northern

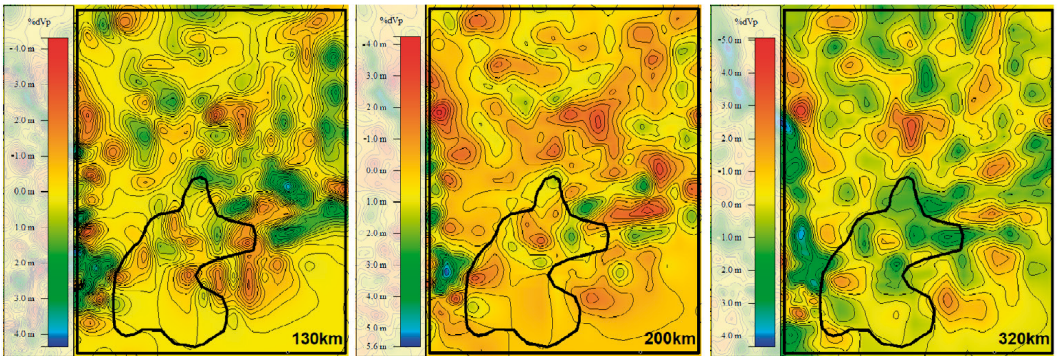

Figure 4 - Panel map of Vp velocity perturbations (dVp Tomography model SAM5_P_2019) at 130 km, 200, and 300 Km depth. The high-speed zone is manifested in forms of islands within the delimited the inferred Cratonic SCLM beneath Central South America; in the extreme north of the aforementioned being more expressive (that coincides with the Paraguayan territory) than in the extreme south, which is more represented by low-speed zones (that coincides with the Uruguayan and Argentine territory).

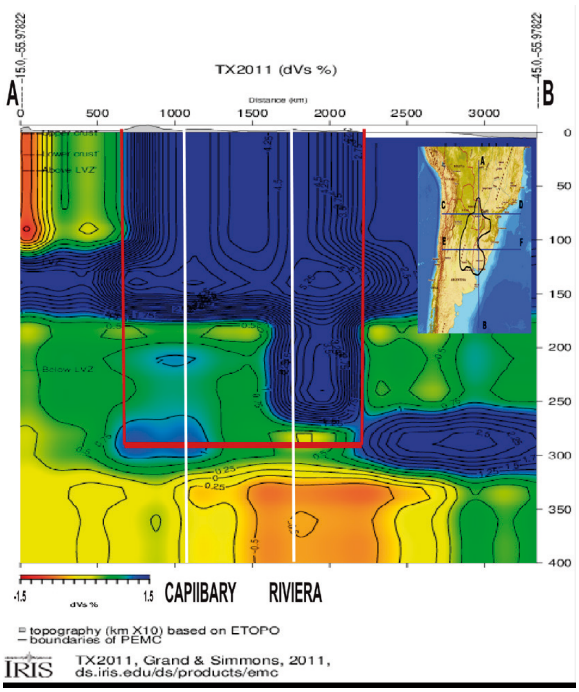

Figure 5 - Cross-section from the N-S line (A-B in the small figure on the right side) of Vs velocity perturbations (dVs% of the TX2011 Tomography model) at 0 to 400 Km of depth, which cuts part of the delimited the inferred Cratonic SCLM beneath Central South America (shown in purple line); that extends up to 300 km deep - cratonic seismic keel. The vertical line of white color to the N representing the intrusion of diamond-bearing lamproite in the north of Paraguayan territory. While the vertical line of the same tone to the south, the intrusion of diamond-bearing lamprophyres from Riviera in Uruguayan territory. We can notice 2 different sets within the delimited craton: 1-north with a strong blue zone up to 180 km deep and from there up to 300 km the speed decreases. 2-south with strong blue-zone continues up to 275/280 km of depth, under which and even its keel a very low-speed zone stands out. And between the two, half-speed fractions. To this middle point, Presser (2016c) attributed it as due to a paleo belt that would have existed in the Archaeozoic; would be two cratonic blocks fused (accreted terranes) from the Archaeozoic.

end of the Rio de la Plata SCLM Craton environment. In this area of the Rio de la Plata SCLM Craton environment, the works of Rocha (2003), Rocha *et al.* (2011 and 2019) and Azevedo *et al.* (2015) show that high % P-wave, speeds that extend to a depth of around 700 km.

Figures 5, 6, 7, and 8 represent a cross-section of S-wave (Figures 5 and 7) and P wave (Figures 6 and 8) that cut the Rio de la Plata SCLM Craton environment in 3 directions. In these figures, the lateral edges of the Rio de la Plata SCLM Craton environment and the inferred seismic cratonic keel are highlighted. The TX2011 Tomography model shows very well the zone of high to moderately dVs speed that extends up to 300 km in-depth, the cratonic root or "keel", below which the low-velocity zone (LVZ) is robust. Something that is little or nothing evident with the dVp Tomography model SAM5_P_2019 information, Figures 6 and 8. However, the lateral limits of the craton in the combination of both seismic tomographic models are clearly highlighted in the aforementioned figures (This was repeated from grade to grade through 12 profile lines; the result being constant as before commented). This information of Figures 5 to 6 are in general agreement with regional seismic studies of several other cratonic regions; which suggest (seismic) *Archon* keel thicknesses as great as 300 km in some area.

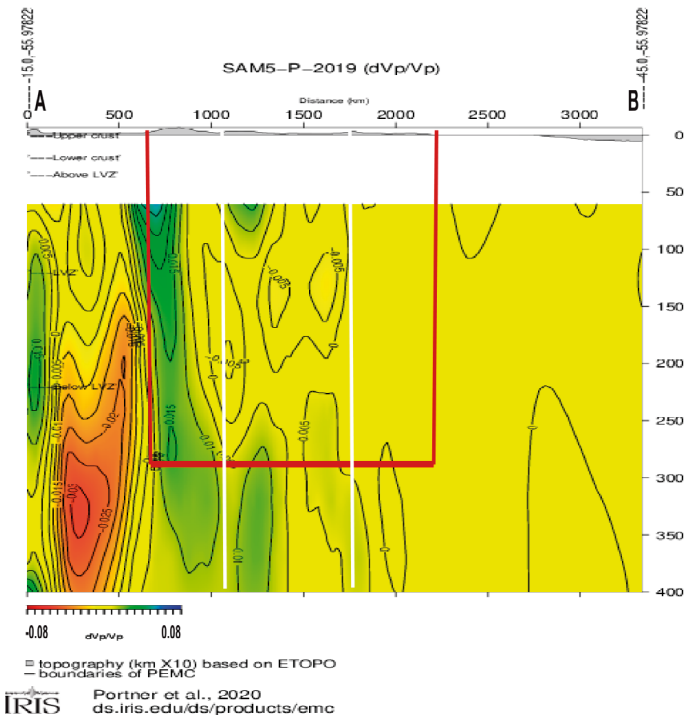

Figure 6 - Cross-section as in Figure 5, but her Vp velocity perturbations (dVp% of the Tomography model SAM5_P_2019). Here the northern edge of the inferred craton is highlighted, while its southern edge shows no definition. Note the highlight tongue of high speed in the north, right in the area of the diamond-bearing lamproite intrusions in Paraguay. This Vp velocity also does not resolve the seismic keel.

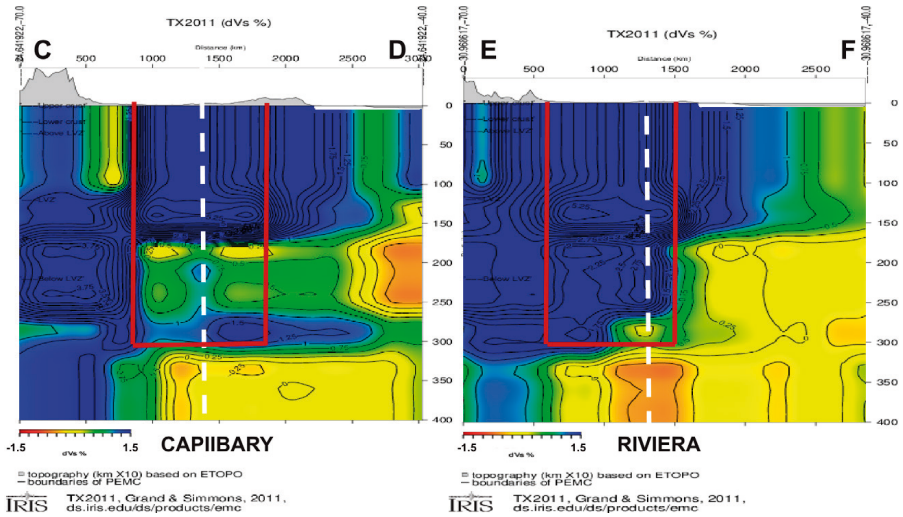

Figure 7 - Cross-section from the E-W line (C-D and E-F in the small figure on the right side) of the same seismic tomography information of Figure 5. And also, here, at 0 to 400 Km of depth, which cuts part of the delimited the inferred Cratonic SCLM beneath Central South America (shown in purple line); that extends up to 300 km deep - cratonic seismic keel. Note in C-D the vertical line of white color, here in dashed line, representing the Capiibary diamond-bearing lamproite intrusions field in Paraguay, a medium-high speed drop-shaped -the filling of a sandwich with a much lower speed (areas that could be due to levels of eclogites or levels that have been metasomatized, see comments in the text). In E-F the vertical dashed line of white color, represents the position of the diamond-bearing Riviera lamprophyres.

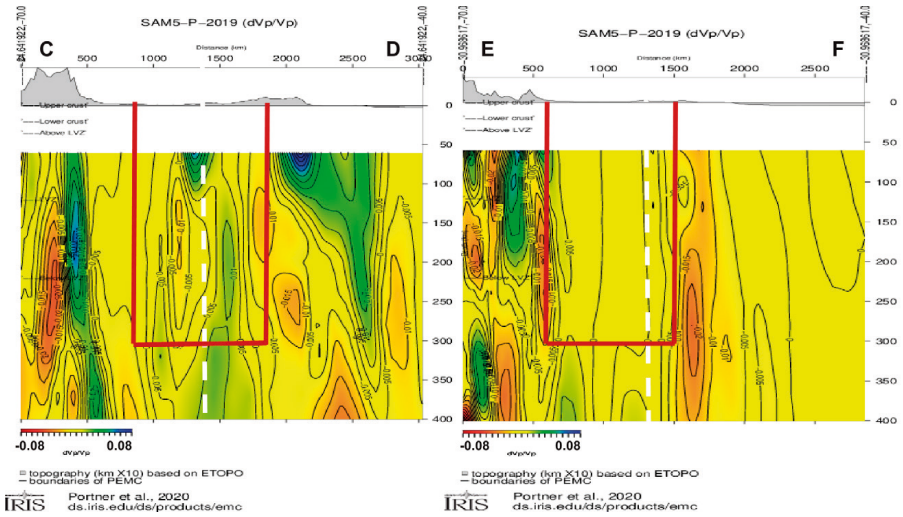

Figure 8 - Cross-section as in Figure 7, also her Vp velocity perturbations (dVp% of the Tomography model SAM5_P_2019). In C-D the edges of the inferred Cratonic SCLM are hinted, clear to the E and less clear to the W. Observe how a high-speed vertical tongue is located next to the intrusion of diamond-bearing lamproites intrusions field in Paraguay. In E-F the edges of the inferred Cratonic SCLM are very well hinted Also here, the same type of vertical line in the previous figure represents the position of the diamond-bearing Riviera lamprophyres. As already commented in Figure 6, the Vp velocity also does not resolve the seismic keel.

Geotherm constraints

Cratons are characterized by both low heat flow and a very low geothermal gradient relative to the Proterozoic mantle (Fouch *et al*., 2004 and references). Presser (2020) inferred, based on 1D Vs profiles (Moulik and Ekstrom, 2014 model), the punctual-mantle geotherm (or mantle geothermal gradient) for 208 points surrounding the previous estimated Rio de la Plata SCLM Craton (core) environment; thus is, values of mantle peridotitic geotherms with 38.5/39 to 43 mW/m^2 and geotherm values of more typical of the of mobile belts area (≥45mW/m^2). At present, 34 more points are added around the area indicated in the new delimited Rio de la Plata SCLM Craton environment beneath Central South America (Figures 3 and 4) and shown in Figure 9.

The distribution of points in Figure 9, also as previously found by Presser (2020), shows mantle geotherm zoning. With the coldest part located at the NNW end of the delimited Rio de la Plata SCLM Craton environment (Figure 3 and 4): 38.5/39-40 mW/m^2 bordered

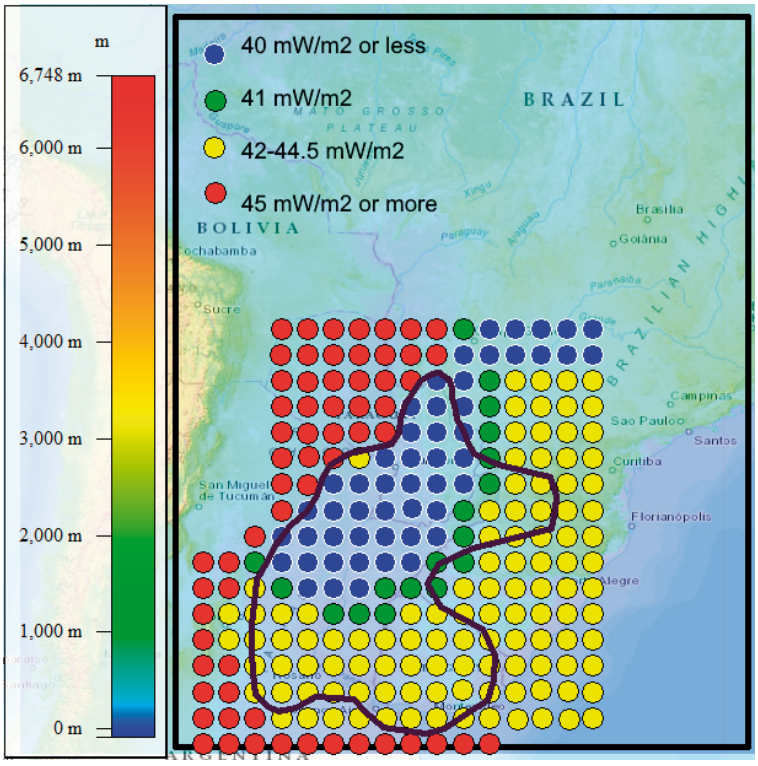

Figure 9 - Map of the inferred Cratonic SCLM beneath Central South America, as the Figures 3 and 4, with estimated general mantle geotherm. Cratonic geotherm as balls of blue, green, and yellow balls; were mobile belts zone is shown in red balls. Here is an upgrade of the Work of Presser (2020) with 242 points of estimated geotherm data. The distribution of points shows mantle geotherm zoning. With the coldest part located at the NNW end of the delimited Rio de la Plata SCLM Craton environment: 38.5/39-40 mW/m^2 bordered by a strip of 41 mW/m^2 and it is weathered by 42-44.5 mW/m^2. Non-cratonic environment: ≥45mW/m^2 to the NW-W-S is evidenced. It can be seen in the Figure how at the NNE end there is also a cold geothermal mantle area, it is believed this is due to the cratonic nucleus raised by Cordani *et al.* (1984).

to the east by a strip of 41 mW/m^2 (both zone distributed between Eastern Paraguay to the NNE of Argentina and portions of SW Brazil) and it is weathered by 42-44.5 mW/m^2 (more properly for Brazilian to Uruguayan territory and less from Argentina territory); while at W-SW-S contrasted by typical high values of the non-cratonic environment: 45mW/m^2 to higher (Area between the NW-W of the Chaco territories in Paraguay and Argentina, to above the Sierras de Cordoba and the La Plata province, Argentina).

Gravimetry Constraints

The "cratonic keels" lack a distinct gravity anomaly and thus appear to be in isostatic equilibrium (Garbert *et al.*, 2018 and references); where gravity anomalies (Bouguer, Free Air) are typically used to constrain crustal densities and geometries (Afonso *et al.*, 2016). Also, the satellite gravity data are a unique source of information on the density structure of the Earth due to its global and relatively uniform coverage. (Afonso *et al.*, 2016).

Respect to the Rio de la Plata SCLM Craton environment some relevant gravimetric information are found in Vidotti *et al.* (1998); Mantovani *et al.* (2005); Mariani (2012); Mariani *et al.* (2012); Dragone *et al.* (2017).

Next, some relevant aspects of the gravimetry of Isostasy, Bouguer of the Rio de la Plata SCLM Craton environment, and between the comments on the cortical thickness of the Rio de la Plata SCLM Craton environment.

Free Air gravity, has been left aside because it would be rather configuring rocks that cover the crystalline basement (*cf*. Presser *et al.*, 2019).

Isostasy

Presser (2014, 2016a and b; 2017; *cf*. also Presser *et al.*, 2016; 2019) obtained the Depth/iso-depths of the crystalline basement domain through the empirical formula: Depth (m.) = -5006.3+(144.1*G), where G is the value of isostasy in mGal. How much this empirical formulation better highlights the crustal characteristics as she is shown in Figure 10;

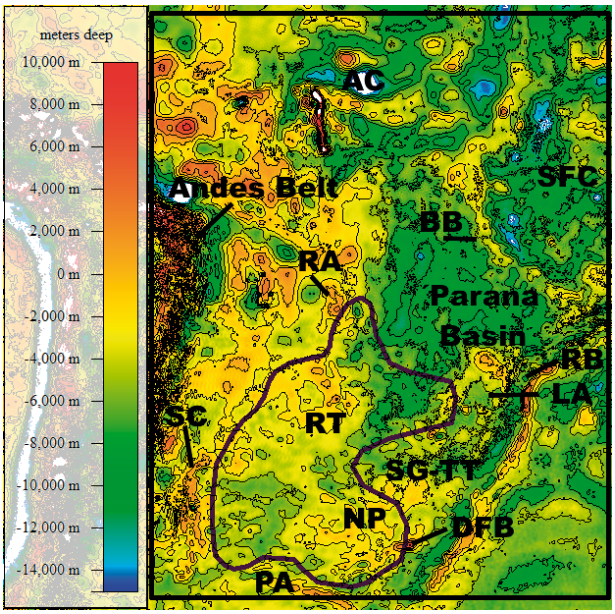

Figure 10 - Panel map of Isostasy gravity as depths/iso-depths of the crystalline basement (Presser, 2014; 2016a and b; see also Presser *et al.*, 2016; 2017 and 2019) for the of the inferred Cratonic SCLM beneath Central South America (As Figures 3 and 4). We can be perceived that it constrained the edges of the Rio de la Plata SCLM Craton environment; this thanks to the high (most shield-area) and some low. The configuration, on its western edge, coincides not far from that drawn in Ramos *et al.* (2010). The most commonly referred surface tectonic units are indicated; as PA, Piedra Alta terrain; SR, Sierra de Córdoba; NP, Nico-Pérez terrain; SG-TT, Sao Gabriel Tacuarembó terrain; RT, Río Tebicuary uplift; RA, Río Apa shield; LA, Luis Alves shield; SFC, Sao Francisco craton; AC, Amazonas craton DFB, don Feliciano Belt; BB, Brasilia Belt and RB, Ribiera Belt. Isostasy data from Bonvalot *et al.*, (2012).

and in it, the most outstanding shield (etc.) are highlighted.

Reviews of the different concepts and forms of the Rio de la Plata craton, whether in its approach to surface geology or some geophysical details can be found in the works of Siegesmund *et al.* (2018); Santos *et al.* (2019); Rocha *et al.* (2019); Dragone *et al.* (2017); Affonso *et al.* (2020); Azevedo (2017); Cunha *et al.* (2019); among others. The discussion about which Rio de la Plata craton different concepts, forms, and supporting criteria are beyond the focus that is intended for this work.

Figure 10, if observed with care can be perceived that is constrained the edges of the Rio de la Plata SCLM Craton environment; this thanks to the high (most shield-area) and some low. Featured by the depth isolines; with the largest depressed area located at NE (of the inferred Cratonic SCLM), it corresponds to the domain of Paraná Basin. And the high coinciding with some shield situated in the RT and NP areas, Figure 10.

Bouguer

Since Bouguer gravity anomalies have a strong link with a depth of crust-mantle boundary, one with positive Bouguer anomalies may mean that it has a thinner crust composed of lower density material and is influenced more strongly by the denser mantle, and vice versa (Neumann *et al.*, 2004); i.e. Bouguer anomalies are indirectly sensitive to crustal thickness, as shown for example in Assumpção *et al.* (2013).

In Figure 11 the Bouguer gravity for the of the inferred Cratonic SCLM beneath Central South America (As Figures 3 and 4). Her as we can see strong contrasts of Bouguer anomaly are not observed; that is, the isoline lines modestly accompany the edges of the inferred Cratonic SCLM. And so, it shows that the Bouguer gravimetric information seems less sensitive to constrained the edges of the inferred Cratonic SCLM beneath Central South America. And as ready commented, the "cratonic

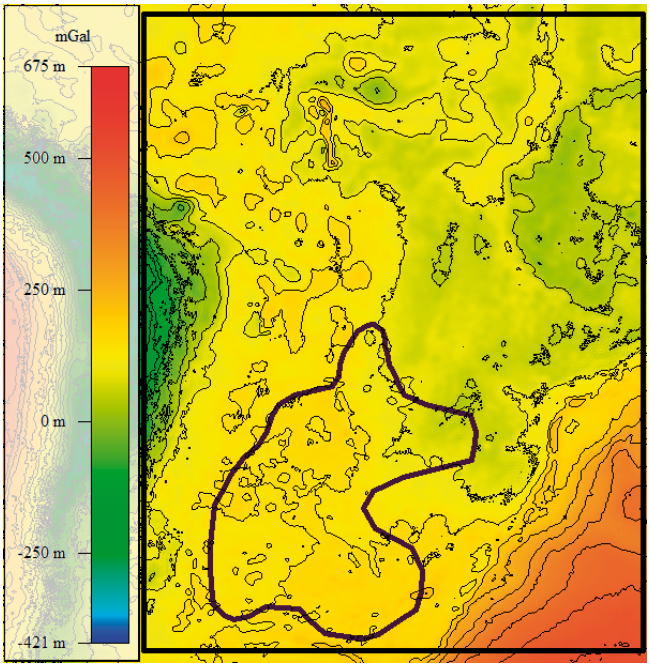

Figure 11- Bouguer gravity map for the of the inferred cratonic SCLM beneath Central South America (As Figures 3 and 4). It is showing an almost uniform behavior inside the inferred Rio de la Plata SCLM Craton environment; that is, strong contrasts of Bouguer anomaly are not observed, with somewhat negative anomalies in the domains of the Paraná basin and positive anomalies related rather to some shield situated in the RT and NP areas, as the Figures 10. Bouguer data from Bonvalot *et al.*, (2012).

keels" lack a distinct gravity anomaly (Garbert *et al.*, 2018 and references).

Crustal Thickness Constraints

Concerning the crustal thickness (CT) of Central South America, there are innumerable jobs; as of Dragone *et al.* (2017 and references); material more than anything relevant to the South American continent. Universal application data can be extracted from CRUST 1.0 model. Modeling that was touched and represented in Figure 12.

CRUST1.0 indicates that the crust beneath the inferred Rio de la Plata SCLM Craton environment is approximately 41 km thick (or 41.000 meters thick) and more properly in the middle-center to the north, and a marked decrease in the SSE, Figure 12. Between the thickest area highlights a small semi-circular region of CT decrease and this is due to the effect produced by a meteorite impact that would have created the San Miguel Impact Crater (Presser *et al.*, 2016).

Magnetometry Constraints

Representing magnetic field measurements with potential field methods provides models that are important to ascertain to the authenticity of magnetic field features. Likewise, visual inspections provide qualitative insight into the consistency between magnetic anomalies and the known geology. However, both approaches say little about the physical parameters of the sources, except maybe in the former case by testing statistical descriptions of the distribution of magnetization against anomaly power spectra. Quantitative magnetic interpretation involving other geophysical quantities such as geology, gravity, seismicity, heat flow, depth to the Moho etc. can be provided by forward modelling methods (Thébault *et al.*, 2010 and references).

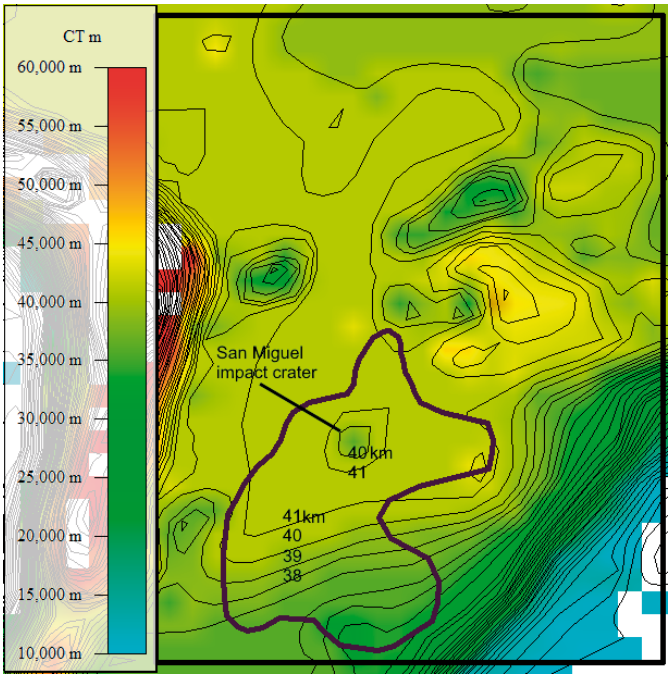

Figure 12 - Crustal thickness (CT) map for the of the inferred cratonic SCLM beneath Central South America (As Figures 2 and 3). The crustal thickness was delineated based on CRUST1.0; which indicates mainly for the area of the inferred craton 41 km thick (41000 meters thick); thick that is thinning to the SSE.

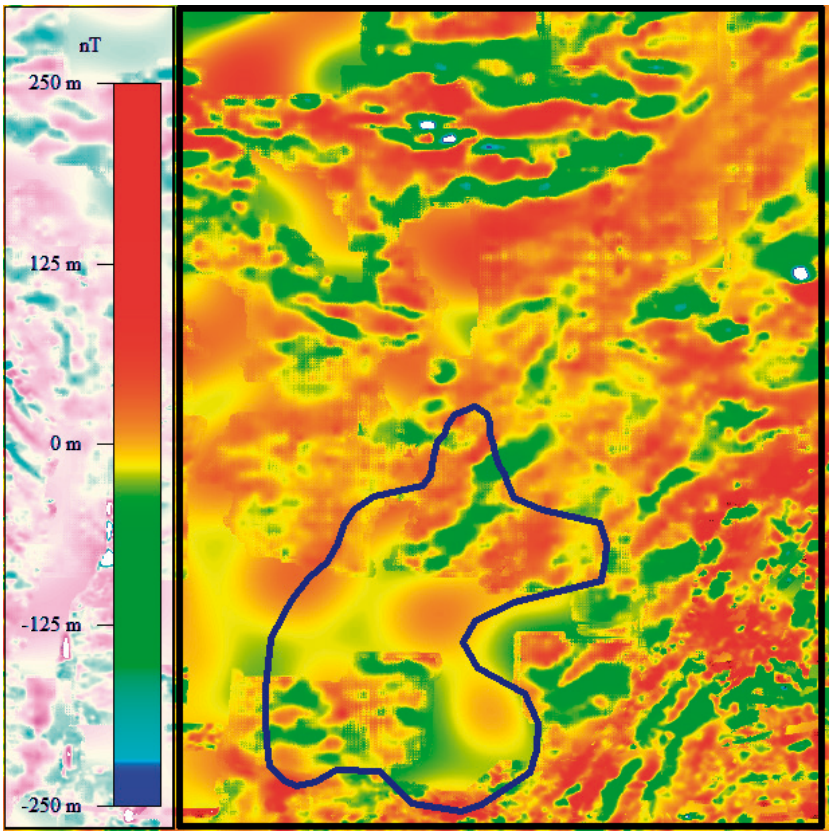

Figure 13 - Magnetic anomaly map (total component) for mixture information obtained from the EMAG 2v3 models, WDMAM 2, and Compilation Getech. Note as this is the resulted information of the magnetic anomaly that highlights the edges of the inferred Cratonic SCLM beneath Central South America (As Figures 2 and 3)

To finish and very briefly, evaluate if the magnetic information could help to constraint the inferred Cratonic SCLM beneath Central South America, we combined the EMAG 2v3 models, WDMAM 2, and Compilation Getech and this is the information of the magnetic anomaly map is shown in Figure 13. The result was satisfactory and it can be seen how magnetic anomalies (especially magnetic high) accompany the edges of the inferred Rio de la Plata SCLM Craton environment.

As well as, important and successful support on the edges and depth of the Rio de la Plata SCLM Craton can also be rescued from the work on magnetotelluric carried out by Favetto *et al.* (2008 and 2015); Pomposiello *et al.* (2011); Orozco *et al.* (2013); Peri *et al.* (2015) and Bologna *et al.* (2018).

DISCUSSION

Changes in elastic and non-elastic properties of mantle rocks measured in indirect seismological studies provide the basis for definitions of the base of the seismic lithosphere. "Seismic lithosphere" is one of the most diverse categories of lithosphere defi-

nitions. According to the classical definition, the seismic lithosphere, or the lid, is a seismic high-velocity layer above the LVZ or above a zone of high velocity gradient in the upper mantle, presumably caused by partial melting (Artemieva, 2011).

The definition of the Cratonic SCLM beneath Central South America as accurately, as possible was made, from the dVs% of the Tomography TX2011 model (Figure 3; the high-speed zones equal to or greater than 4.3 dVs%), which was reinforced with the dVp Tomography model SAM5_P_2019 (Figure 4, 5, 6, 7 and 8). Thus, was obtaining an undoubted constraint of the edges of the Cratonic SCLM beneath Central South America. Limits of the Cratonic SCLM that were released in gravimetric information (Figures 10 and 11; with excellent definition in isostasy), magnetometric configuration (Figure 13) in addition to the new definition of cratonic mantle geotherm/belt geotherm (in 242 points, Figure 9; 34 new points over 208 points of Presser, 2020) and the highlight of the crustal thickness in that environment (mostly 40 to 41 km., Figure 12). This constrained the Cratonic SCLM beneath Central South America with 1500 kilometers long by 870 to 880 wides in its wider parts, and that extends over a large part of the territories of Paraguay and Uruguay, the northern provinces of Argentina, and fractions of some southern states of Brazil (Figure 3, 4, 9, 10, 12 and 13) was seen as being the Cratonic SCLM heart of the Rio de la Plata Craton.

Figures 5 and 7, but also in some way the Figures 6 and 8, show a cratonic keel as near 300 km depth; i.e. it's "Seismic cratonic keel". This above the robust LVZ (Figures 6 and 8); but pronounced LVZ beneath cratonic lithosphere are rare; where present (South America; Tanzania) they are often neighbored by volcanic areas near cratonic boundaries (Lebedev and van der Hilst, 2010). If also considerate the S-wave and P-wave dates exposed in the works of Rocha (2003) and Rocha *et al*., (2011) as well as in Rocha *et al*. (2019) and Azevedo *et al*. (2015), that show very deep high-speed zones as S and P-wave in some portion of the delineated her as the Rio de la Plata SCLM Craton environment, the analysis would allow concluding that these data's are in general agreement with that raised by Fouch *et al*. (2004 and references); James *et al*. (2001, 2004); James and Fouch (2002); Begg *et al*. (2009) that found that the strong positive velocity perturbations across the Kalahari craton region that suggest seismically-defined keel extends to depths of ~225 to 300 km beneath the craton

Presser (2020) based on 1D Vs profiles (on 208 numbers of points), inferred cratonic peridotitic mantle geotherms at the Rio de la Plata SCLM Craton environment: 38.5 to 40 mW/m^2 in its central northern portion and southern portion and in its edges/southern portion 40 to 42 mW/m^2. Mantle geotherm values that allowed estimate cratonic keel between 243 to 237 km depth (northern portion) and 225 to 213 km depth (southern portion), this is two accreted blocks as is evident in Figure 5 (see also in Presser, 2016c). This mantle geotherm is upgraded with new 34 points in Figure 9; data that reinforced the seismically inferred deep cratonic keel; and so, as the craton-edges, in the Rio de la Plata SCLM Craton environment.

Seismic tomography and mantle geotherm data show depths of the cratonic keel of more than 200 km deep; so that as commented in the introduction, Presser (2011), states that the LAB depth greater than 193.5 at 195 km would denote ages> 2500 Ma., this estimated from the formula z = 0.04 * t + 93.6 (Artemieva, 2006); so, which would make the statement that the *Archon* craton is extremely correct for the Rio de la Plata SCLM Craton.

As well, in another way, the Paraná central basin basement (Figures 10 and 11)

has a high-density root (i.e., a more fertile subcontinental lithospheric mantle related to Parana Magmatic Province; *cf*. Chaves *et al.*, 2016) and the subcontinental lithospheric mantle below great part the Rio de la Plata SCLM *Archon* Craton environment (W-SW portion of the Parana Basin), as we can be seen in the work of Chaves *et al.* (2016), is with strong low-density root. The low-density root is a typical characteristic of chemically depleted Archean cratons (Chaves *et al.*, 2016).

The plates dVs% and dVp% of Figures 3, 4, 5, 6, 7, and 8 evidence some low-velocity portions below the Rio de la Plata SCLM *Archon* Craton environment. This is thought to be due to it representing probably a level that may be higher in basaltic components (eclogitic) or metasomatized fluids that hydrated and altered the host peridotite, as raised by Shirey et al. (2002) for some P-wave low-velocity zones in the Kaapvaal *Archon* of SCLM and matching kimberlites rich in eclogitic inclusions in their diamonds. Presser and Benitez (2021) found that in the north portion of Rio de la Plata SCLM *Archon* Craton environment, located in Paraguay, with investigated more than 5000 samples of stream sediments, the soil above lamproite pipe anomalies and lamproite/lamprophyres pipe fill material, the presence of garnet grains of eclogitic origin predominate.

Figure 14 shows the Rio de la Plata SCLM *Archon* Craton on a basis of dVs% at 150 km and dVp% at 165 km and in them have launched diamond-bearing kimberlites (and without diamonds), diamond-bearing lamproites (and without diamonds), and diamond-bearing alkaline picritic lamprophyres and some Mesozoic to Tertiary alkaline rocks (the last three occur in Paraguay; *cf*. Presser, 2016c and 2019; Presser *et al.*, 2014; Bitschene, 1987; and others). The dVs% sheet shows how within the portion of the Rio de la Plata SCLM *Archon* Craton in Paraguay it hosts diamond-bearing lamproites and lamprophyres; where some localities yielded data on the formation pressure of typically deep cratonic environments (> 200 km deep as seen in Presser, 2016c; 2020; Presser and Benitez, 2021 and see also Smith *et al.*, 2012; and Presser *et al.*, 2014). For comparisons see also, in the same figure, the information that is appreciated about kimberlites in Brazil (portions of AC and SFC) and Uruguay in the same Figure 14.

Also, in Figure 14, the dVp% sheet illustrates occurrences of lamproites associated with high (Puentesiño) and low (Capiibary, Ybytyruzú, and Riviera) velocity zones within the Rio de la Plata SCLM *Archon* Craton. For comparisons see also, in the same figure, the information that is appreciated about kimberlites in Brazil (Juina cluster and Pimenta Bueno cluster). Details that deserve further study and that are beyond the scope of this writing.

Na-alkaline rocks of the Tertiary and Mesozoic K-alkaline to ultra-potassic rocks occur associated with the rift (Na-alkaline; Bitschene,1987) rift/graben (mainly K-alkaline to ultra-potassic; Bitschene,1987) Structure called the Asuncion rift, which according to Presser (2019 and references) would have been formed as a result of the meteorite impact (which formed the San Miguel impact crater with about 130 km in diameter; Presser *et al.*, 2016).The meteorite impact would have caused, in this area, the crustal thinning of the Rio de la Plata SCLM *Archon* Craton; and so, they would have facilitated the alkaline (non-kimberlitic) magmas and diamond-bearing picritic calc-alkaline lamprophyres and diamond-bearing lamproites magmas intrusion/extrusion in these places.

Finally, it is also necessary to highlight that the limits of the Rio de la Plata SCLM *Archon* Craton on its eastern edges; in Uruguay, the Don Feliciano belt, and Brazil, some portion of the Ribeira belt (Figures 3,

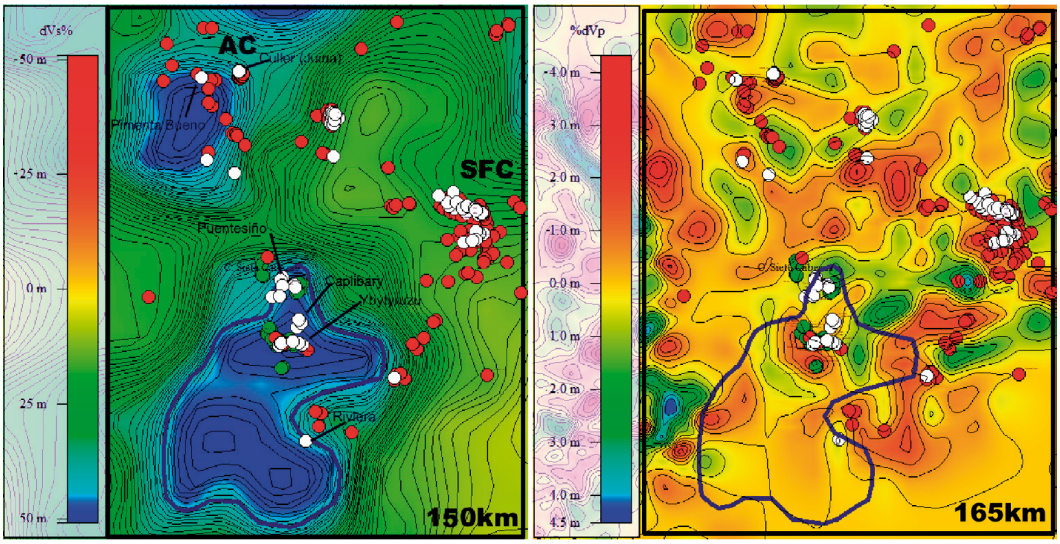

Figure 14 - Map of dVs% at 150 km and dVp% at 165 km of the Rio de la Plata SCLM *Archon* Craton. In them were launched diamond-bearing kimberlites (as white balls) and without diamonds (as red balls). And so as, diamond-bearing lamproites (as white balls) and without diamonds (as red balls) and diamond-bearing picritic calc-alkaline lamprophyres (as white balls) and some Mesozoic to Tertiary alkaline rocks (as green balls); the last tree that occurs in Paraguay; *cf.* Bitschene (1987); Presser (2016c and 2019). In Riviera-Uruguay we know diamond-bearing ultramafic lamprophyres. More comments in the text.

4, and 10) could have been thrust on top of the Rio de la Plata SCLM *Archon* Craton and thus subtract their definition with the geophysics configuration of the Rio de la Plata SCLM *Archon* Craton where the geophysical information in this work contemplated the expression of the mantle rather than the characteristics of the crust. In Paraguay, the area of exposure of rocks of the crystalline basement, commonly known as the Alto del Rio Tebicuary (*cf.* Cordani *et al.*, 2001), is the same area of influence of the San Miguel impact crater, so they remain to be resolved the implications of this impact phenomenon and its probable role in the genesis of some granitoid rocks within its setting.

CONCLUSIONS

The definition of the Rio de la Plata SCLM *Archon* Craton presented focused on delineating its edges based mainly on the geophysical behavior with emphasis on the published S-wave (% dVs global) that is complemented with the published P-wave (% dVp continental). Limits that are reinforced with the (global) gravimetric, (regional) crustal thickness, (regional) mantle geotherm, and (global) magnetometric information.

Geophysics configuration constrains 1500 kilometers long by 870 to 880 wide in its wider parts; i.e., 971513 sq. km. for the Rio de la Plata SCLM *Archon* Craton with seismically defined keel extends to depths of ~280 to 300 km. Rio de la Plata SCLM Archon Craton depths that are in general agreement with global/regional seismic studies of several other Africa Archon cratonic regions (*cf.* Fouch *et al.*, 2004 and references; James et al., 2001 and 2004; James and Fouch, 2002; Begg *et al.*, 2009; Presser, 2020 and Presser and Benitez, 2021).

The geophysical constrained Rio de la Plata SCLM *Archon* Craton delimits to the east approximately with the Cordoba mountain (Pampean range in Pomposiello *et al*., 2011), to the NNW with the Rio Apa shield (*cf*. Teixeira *et al*., 2020), and to the southeast-south, it encompasses a set of shields exposed in Uruguay - bordered further east by the Don Feliciano belt (*cf*. Siegesmund *et al*., 2018 and references) and in the south the Tandilia belt in Argentina (*cf*. Ramos, 1999). However, in this constrained Rio de la Plata SCLM *Archon* Craton shield areas within the domain craton are only known next to Alto del Rio Tebicuary in Paraguay (*cf*. Cordani *et al*., 2001) and the terranes (in Uruguay) Nico Perez, Piedra Alta, Rivera block and Tacuarembó block (*cf*. Rapela *et al*., 2007).

In Paraguayan territory, the Rio de la Plata SCLM *Archon* Craton hosts abundant diamond-bearing lamproitic pipes, diamond-bearing picritic calc-alkaline lamprophyres pipes; while in Uruguay diamond-bearing ultramafic lamprophyres are known.

This work attempt to constrain, first of all, the Rio de la Plata SCLM *Archon* Craton core from Central- South America, some eventual inconsistencies of what was concluded here with the surface geology, therefore, were not taken into consideration.

REFERENCES

Afonso, J.C., Moorkamp, M. and Fullea, J. (2016). Imaging the Lithosphere and Upper Mantle: Where We Are at and Where We Are Going. In Integrated Imaging of the Earth: Theory and Applications, Geophysical Monograph 218, First Edition. Edited by Max Moorkamp, Peter G. Lelièvre, Niklas Linde, and Amir Khan. © 2016 American Geophysical Union. Published 2016 by John Wiley & Sons, Inc. pp. 191-218.

Affonso, G.M.P.C., Rocha, M.P., Costa, I.S.L., Assumpção, M., Fuck, R.A., Albuquerque, D.F., Portner, D.E., Rodríguez, E.E. and Beck, S.L. (2019). Lithospheric architecture of the Paranapanema Block and adjacent nuclei using multiple-frequency P-wave seismic tomography. Volume 126, Issue 4 e2020JB021183.

Artemieva, I.M. (2006). Global 1°×1° thermal model TC1 for the continental lithosphere: Implications for lithosphere secular evolution. Tectonophysics, 416: 245–277.

Artemieva, I.M. (2011). The Lithosphere: An Interdisciplinary Approach. Publisher: Cambridge University Press, ISBN: 978-0-521-84396-6. 794 Pp.

Assumpção, M., Schimmel, M., Escalante, C., Barbosa, J.R., Rocha, M. and Barros, L.V. (2004). Intraplate seismicity in SE Brazil: Stress concentration in lithospheric thin spots. Geophysical Journal International, 159(1): 390–399. https://doi.org/10.1111/j.1365-246X.2004.02357.x

Assumpção, M., Feng, M., Tassara, A. and Julià, J. (2013). Models of crustal thickness for South America from seismic refraction, receiver functions and surface wave tomography. Tectonophysics 609: 82–96.

Assumpção, M., Azevedo, P.A., Rocha, M.P. and Bianchi, M.B. (2017). Lithospheric Features of the São Francisco Craton. In Springer International Publishing Switzerland 2017 Heilbron, M. et al. (eds.), São Francisco Craton, Eastern Brazil, Regional Geology Reviews.

Azevedo, P.A. (2017). Estudo do manto superior sob o Brasil utilizando Tomografia Sísmica de Tempo de Percurso com ondas P. PhD. Thesis Universidade de Brasília.

Azevedo, P.A., Rocha, M.P., Soares, J.E.P. and Fuck, R.A. (2015). Thin lithosphere between the Amazonian and São Francisco cratons, in central Brazil, revealed by seismic P-wave tomography. Geophysical Journal International, 201(1): 61–69. https://doi.org/10.1093/gji/

Begg, G.C., Griffin, W.L., Natapov, L.M., O'Reilly, S.Y., Grand, S.P., O'Neill, C.J., Hronsky, J.M.A., Poudjom Djomani,Y., Swain, C.J., Deen, T. and Bowden. P. (2009). The lithospheric architecture of Africa: Seismic tomography, mantle petrology, and tectonic evolution. *Geosphere*; February 2009; v. 5; no. 1: 23–50; doi: 10.1130/GES00179.1.

Bitschene, P.R. (1987). Mesozoischer und Kanozoischer anorogener magmatismus in Ostparaguay: arbeiten zur geologie und petrologie zweier Alkaliprovinzen, Ph.D. Dissertation, Heidelberg University, Heidelberg, Germany. Ggv003.

Bologna, M.S., Dragone, G.N., Muzio, R., Peel, E., Nuñez-Demarco, P. and Ussami, N. (2018). Electrical structure of the lithosphere from Rio de la Plata craton to Paraná basin: Amalgamation of cratonic and refertilized lithospheres in SW Gondwanaland. Tectonics, 37. https://doi.org/10.1029/2018TC005148.

Bonvalot, S., Balmino, G., Briais, A., M. Kuhn, Peyrefitte, A., Vales, N., Biancale, R., Gabalda, G., Reinquin, F. and Sarrailh, M. (2012). World Gravity Map. Commission for the Geological Map of the World. Eds. BGI-CGMW-CNES-IRD, Paris.

Celli, N.L., Lebedev, S., Schaeffer, A.J. and Gaina, C. (2020). African cratonic lithosphere carved by mantle plumes. Nature Communications, 11:92.

Chaves, C., Ussami, N. and Ritsema, J. (2016). Density and P-wave velocity structure beneath the Parana Magmatic Province: Refertilization of an ancient lithospheric mantle, Geochem. Geophys. Geosyst., 17, 3054–3074, doi:10.1002/2016GC006369.

Cordani, U.G., Brito Neves, B.B., Fuck, R., Porto, R., Filho, A. and Da Cunha, F.M.B. (1984). Estudo preliminar de integração do Pré-Cambriano com os eventos tectônicos das bacias sedimentares brasileiras. Ciência Técnica Petróleo, 15 Pp.

Cordani, U.G., Cubas, N., Sato, K., Nutman, A.P., Gonzales, M. and Presser, J.L.B. (2001). Geochronological constraints for the evolution of the metamorphic complex near the Tebicuary River. In: Southern Precambrian Region of Paraguay. III Simposio Sudamericano de Geologia Isotopica, Pucon – Chile.

Cunha, A., Zálan, P.V., Adriano, L., Sousa Neves, A., Perosia, F.A., Hidalgo-Gatoe, M., La Terra, E., Fontes, S., Silva, D. and Adriano. M. (2019). Analyzing the gravity response of the Serra Geral Basalts and its impacts for the gravity interpretation in the northern Paraná Basin. Journal of South American Earth Sciences 89: 259–274.

Dragone, G.N., Ussami, N., Gimenez, M.E., Lince Klinger, F.G. and Chaves, C.A.M. (2017). Western Paraná suture/shear zone and the limits of Rio Apa, Rio Tebicuary and Rio de la Plata cratons from gravity data. Precambrian Research, 291, 162–177. https://doi.org/10.1016/j.precamres.2017.01.029.

Favetto, A., Pomposiello, C., López de Luchi, M. and Booker, J. (2008). 2D magnetotelluric interpretation of the crust electrical resistivity across the Pampean terrane-Río de la Plata suture, in central Argentina. Tectonophysics, 459, 54-65.

Favetto, A., Rocha, V., Pomposiello, C., García, R. and Barcelona, H. (2015). A new limit for the NW Río de la Plata Craton Border at about 24ºS (Argentina) detected by Magnetotellurics Geologica Acta: an international earth science journal, vol. 13, núm. 3: 243-254.

Faure, S., Godey, S., Fallara, F. and Trépanier, S. (2011). Seismic Architecture of the Archean North American Mantle and its Relation to Diamondiferous Kimberlite Fields. Geology, v. 106: 223–240.

Fouch, M.J., James, D.E., VanDecar, J.C., van der Lee, S. and The Kaapvaal Seismic Group, 2004. Mantle seismic structure beneath the Kaapvaal and Zimbabwe Cratons: South African Journal of Geology, v. 107: 33–44.

Garber, J.M., Maurya, S., Hernandez, J.A., Duncan, M.S., Zeng, L., Zhang, H.L., Faul, U., Mccammon, C., Montagner, J., Moresi, L., Romanowicz, B., Rudnick, R. and Stixrude, L. (2018). Multidisciplinary constraints on the abundance of diamond and eclogite in the cratonic lithosphere. *Geochemistry*, *Geophysics*, *Geosystems*, 19. https://doi.org/10.1029/2018GC007534.

Grand, S.P. (2002). "Mantle Shear-Wave Tomography and the Fate of Subducted Slabs." Phil. Trans. R. Soc. Lond. 360: 2475-2491.

James, D.E., Fouch, M.J., VanDecar, J.C., van der Lee, S. and the Kaapvaal Seismic Group. (2001). Tectospheric structure beneath southern Africa. Geophysical Research Letters, 28: 2485-2488.

James, D.E. and Fouch, M.J. (2002). Formation and evolution of Archaean cratons: insights from southern Africa. In: C. M. R. Fowler, C. J. Ebinger and C. J. Hawkesworth (Editors), Early Earth: Physical, Chemical and Biological Development, Special Publication of the Geological Society of London, 199: 1-26.

James, D., Boyd, F., Schutt, D., Bell, D. and Carlson, R. (2004). Xenolith constraints in seismic velocities in the upper mantle beneath southern Africa. Geochem. Geophys. Geosys. 5, doi:10.1029/2003GC000551.

Janse, A.J.A. (1994). Is Clifford's Rule still valid? Affirmative examples from around the world: In H.O.A. Meyer and O.H. Leonardos (eds) Proceedings of the Fifth International Kimberlite conference 2, Diamonds: Characterization, Genesis and Exploration. Brasilia: CPRM Special Publication IB, p. 215-235.

Janse, A. (1998). Archons, protons and tectons: an update. International Kimberlite Conference: Extended Abstracts, 7(1): 377–379.

Lebedev, S. and van der Hilst, R.D. (2010). (MIT) S-Velocity Structure of the Upper Mantle IRIS Core Proposal | Volume II | Upper Mantle Structure and Dynamics | II -169.

Lesur, V., Hamoudi, M., Choi, Y., Dyment, J. and Thebault, E. (2016). Building the second version of the World Digital Magnetic Anomaly Map (WDMAM), Earth, Planets and Space 68:27 DOI 10.1186/s40623-016-0404-6.

Mantovani, M.S.M., Quintas, M.C.L., Shukowsky, W. and Brito Neves, B.B. (2005). Delimitation of the Paranapanema Proterozoic block: A geophysical contribution. *Episodes*, *28*(1): 18–22.

Mariani, P. (2012). Caratterizzazione della struttura litosferica del bacino intracratonico del Paranà (Sud

America) mediante modellazione di dati gravimetrici da satelliti di nuova generazione (GRACE e GOCE). Ph.D. thesis. Università degli Studi di Trieste, Italy.

Mariani, P., Braitenberg, C. and Ussami, N. (2013). Explaining the thick crust in Paraná basin, Brazil, with satellite GOCE gravity observations. Journal of South American Earth Sciences 45: 209-223.

Moulik, P. and Ekström, G. (2014). An anisotropic shear velocity model of the Earth's mantle using normal modes, body waves, surface waves and long-period waveforms. Geophysical Journal International, 199 (3): 1713-1738.

Neumann, G.A., Zuber, M.T., Wieczorek, M.A., Mc Govern, P.J., Lemoine, F.G. and Smith, D.E. (2004). "Crustal structure of Mars from gravity and topography". Journal of Geophysical Research: Planets. 109 (E8): E08002.

Orozco, L.A., Favetto, A., Pomposiello,C., Rossello, E. and Booker, J. (2013). Crustal deformation of the Andean foreland at 31° 30'S (Argentina) constrained by magnetotelluric survey. Tectonophysics 582: 126–139.

Peri, V.G., Barcelona, H., Pomposiello, M.C. and Favetto, A. (2015). Magnetotelluric characterization through the Ambargasta-Sumampa Range: The connection between the northern and southern trace of the Río de La Plata Craton-Pampean Terrane tectonic boundary. Tectonophysics, 59: 1-12.

Pomposiello, C., Favetto, A., Peri, V.G., Barcelona, H. and Orozco L.A.B. (2011). Magnetotelluric Study In The Western Border Of The Río De La Plata Craton (Chacopampeana Plain And Eastern Sierras Pampeanas). Latinmag Letters, Volume 1, Special Issue (2011), A18: 1-7. Proceedings Tandil, Argentina.

Portner, D.E., Rodríguez, E.E., Beck, S., Zandt, G., Scire, A., Rocha, M.P., (2020). Detailed structure of the subducted Nazca slab into the lower mantle derived from continent-scale teleseismic P wave tomography. Journal of Geophysical Research: Solid Earth, 125, e2019JB017884. https://doi.org/https://doi.org/10.1029/2019JB017884.

Presser, J.L.B., 2011. Distinción Sismológica entre el manto Arqueozoico y el Proterozoico: la raíz de la litosfera bajo la Cuenca del Paraná, América del Sur. Reportes Científicos de la Facen, 2(1): 45-72.

Presser, J.L.B., (2014). Configuración del escenario geológico de la región occidental. (Inédito), DOI: 10.13140/RG.2.1.4291.4728.

Presser, J.L.B. (2016a). Geología de la Reserva Natural Tapyta (Departamento de Caazapá) Paraguay. Informe interno: Organización No Gubernamental Agua – ONGAGUA CONACYT/Prociencia, Asunción Paraguay. 90 pp.

Presser, J.L.B. (2016b). Muy Probables Mega Estructuras De Impacto En Paraguay: I- El Chaco. Reporte Científicos Facen, 7(1): 5-13.

Presser, J.L.B. (2016c). Diamantes en Paraguay, Cincuenta Años de Ocurrencia. Bol. Mus. Nac. Hist. Nat. Parag. Vol. 20, nº 2: 154-187.

Presser, J.L.B. (2019). El lamprófido picrítico con diamantes Ymi-1. Pyroclastic Flow, 9(1): 23-34.

Presser, J.L.B., (2020). Rio de la Plata Archon Craton-Core peridotitic geotherms. Historia Natural, 10 (3) 2020: 5-16.

Presser, J.L.B., Bitschene, P. R. and Vladykin, N.V. (2014). Comentarios Sobre La Geología, La Petrografía Y La Química Mineral De Algunas Lamproítas De La Porción Norte De La Cordillera Del Ybytyruzú, Paraguay Oriental. Bol. Mus. Nac. Hist. Nat. Parag. 18(1): 24-61.

Presser, J.L.B., Bulanova, G.P. and Smith, C.B. (2014). Diamantes De Capiibary, Dpto. San Pedro, Paraguay. Boletin del Museo Nacional de Historia Natural del Paraguay, 18(1): 5-23.

Presser, J.L.B., Fariña-Dolsa, S., Larroza, F.A.C., Rocca, M., Alonso, R.N., Acevedo, R.D., Cabral-Antúnez, N.D., Baller, L., Zarza-Lima, P.R. and Sekatcheff, J. M. (2016). Modeled mega impact structures in Paraguay: II- the Eastern region**.** Boletín del Museo Nacional de Historia Natural del Paraguay 20(2): 205-213.

Presser, J.L.B., and ONGAgua. (2017). Formación Patiño: Fundamentos del modelado geofísico. Reporte interno, 12 pp.

Presser, J.L.B., Vladykin, N.V., Bitschene, P.R., Tondo, M. J., Acevedo, R.D., Alonso, R. and Benitez, P. (2017). Olivino-lamproita del Campo de Lamproitas Ybytyruzú, Paraguay Oriental. Pyroclastic Flow, 7 (1): 1-15.

Presser, J.L.B., Alonso, R. and Rocca M. (2019). Malvinas Islands (Falkland Islands): Advances in the inferred buried marine impact mega-structure. Pyroclastic Flow, 9 (1): 1-14.

Presser, J.L.B. and Kumar, S.K. (2020). The Bunder lamproitescluster (India): tectonics, lithospheric mantle and environment -a review. *Pyroclastic Flow*, 10(1): 1-9.

Presser, J.L.B and Benitez, P. (2021). Eclogitic geotherms of the Río de la Plata craton archon-core: Estancia Trementina and Puentesiño, Dpto. of Concepción -Paraguay. Compared to two large diamond deposits Argyle (lamproitic) and Orapa (kimberlitic). Historia Natural Cuarta Serie Volumen 11 (2) *in this numer*.

Ramos, V. (1999). Rasgos Estructurales Del Territorio Argentino: 1. Evolucion Tectónica De La Argentina. Anales 29 (24): 715-784, Buenos Aires.

Ramos, V.A., Vujovich, G., Martino, R. and Otamendi, J. (2010). Pampia: A large cratonic block missing in

the Rodinia supercontinent. Journal of Geodynamics, 50: 243–255.

Rapela, C.W., Fanning, C.M., Casquet, C., Pankhurst, R.J., Spalletti, L., Poiré, D. and Baldo, E.G. (2011). The Rio de la Plata craton and the adjoining Pan-African/brasiliano terranes: heir origins and incorporation into south-west Gondwana. *Gondwana Research*, *20*(4): 673–690. https://doi.org/10.1016/j.gr.2011.05.001.

Rocha, M.P. (2003). Ampliação da Tomografia Sísmica do Manto Superior no Sudeste e Centro-Oeste do Brasil com ondas P, M.Phil thesis – IAG-USP, São Paulo.

Rocha, M.P., Schimmel, M. and Assumpção, M. (2011). Upper-mantle seismic structure beneath SE and Central Brazil from P and S-wave regional traveltime tomography. Geophysical Journal International, 184(1): 268–286.

Rocha, M.P., de Azevedo, P.A., Marotta, G.S., Schimmel, M. and Fuck, R. (2016). Causes of intraplate seismicity in central Brazil from travel time seismic tomography. Tectonophysics, 680: 1–7. https://doi.org/10.1016/j.tecto.2016.05.005

Rocha, M.P., Assumpção, M., Affonso, G.M.P.C., Azevedo, P.A. and Bianchi, M. (2019). Teleseismic P-wave Tomography Beneath the Pantanal, Paraná and Chaco-Paraná Basins, SE South America: Delimiting Lithospheric Blocks of the SW Gondwana Assemblage. Journal of Geophysical Research: Solid Earth, 124, 2018JB016807. https://doi.org/10.1029/2018JB016807

Rosa, M. L., Collaço, B., Assumpção, M., Sabbione, N. and Sánchez, G. (2016). Thin crust beneath the Chaco-Paraná Basin by surface-wave tomography. Journal of South American Earth Sciences, 66: 1–14. https://doi.org/10.1016/j.jsames.2015.11.010

Schimmel, M., Assumpção, M. and VanDecar, J. C. (2003). Seismic velocity anomalies beneath SE Brazil from P and S wave travel time inversions. Journal of Geophysical Research, 108(B4), 2191. https://doi.org/10.1029/2001JB000187

Santos, J.O., Chernicoff, C.J., Zappettinid, E.O., McNaughtone N.J. and Hartmann, L.A. (2019). Large geographic and temporal extensions of the Río de la Plata Craton, South America, and its metacratonic eastern margin. International Geology Review 2019, VOL. 61, NO. 1: 56–85.

Shirey, S.B., Harris, J.W., Richardson, S.H., Fouch, M.J., James, D.E., Cartigny, P., Deines, P. and Viljoen, F. (2002). Diamond Genesis, Seismic Structure, and Evolution of the Kaapvaal-Zimbabwe Craton. Science Vol 297: 1683-1686.

Siegesmund, S., Stipp Basei, M.A., Oyhantçabal, P. and Oríolo, S. (2018). Geology of Southwest Gondwana. Cham, Switzerland, Springer International Publishing. 700 pp.

Smith, C.B., Bulanova, G.P. and Presser, J.L.B. (2012). Diamonds From Capiibary, Paraguay. 10th International Kimberlite Conference Extended Abstract No. 10IKC-36.

Teixeira, W., Cordani, U.G., Faleiros, F.M., Sato, K., Maurer, V.C., Ruiz, A.S. and Azevedo, E.J.P. (2020). The Río Apa Terrane reviewed: U-Pb zircon geochronology and provenance studies provide paleotectonic links with a growing Proterozoic Amazonia. Earth-Science Reviews, 202, 1-35.

Thébault, E., Purucker, M., Whaler, K. A., Langlais, B. and Sabaka, T.J. (2010). The Magnetic Field of the Earth's Lithosphere. Space Sci. Rev. DOI 10.1007/s11214-010-9667-6.

Vidotti, R.M., Ebinger, C.J. and Fairhead, J.D. (1998). Gravity signature of the western Paraná Basin. Earth and Planetary Science Letters 159: 117-132.

Recibido: 24/04/2021 - Aceptado: 03/06/2021 - Publicado: 30/07/2021